Slow Dynamics of Consolidated Granular Systems: Multi-scale Relaxation

Parisa Shokouhi[a], Jacques Rivière[b], Robert A. Guyer[c], and Paul A. Johnson[c]

[a]Department of Civil and Environmental Engineering, Pennsylvania State University, 215 Sackett Building, University Park, PA 16802, USA

[b]University Grenoble Alpes, CNRS, Institute of Earth Sciences (ISTerre), 38000 Grenoble, France

[c]Los Alamos National Laboratory, MS D446, Los Alamos, NM 87545, USA

ABSTRACT

Dynamic acousto-elastic testing, a pump-probe scheme, is employed to investigate the recovery of consolidated granular media systems from the non-equilibrium steady state established by a pump strain field. This measurement scheme makes it possible to follow the recovery from the non-equilibrium steady state over many orders of magnitude in time. The recovery is described with a relaxation time spectrum that is found to be independent of the amplitude of the non-equilibrium steady state (pump amplitude) and of the environment in which samples reside. The non-equilibrium steady state and its slow recovery are the laboratory realization of phenomena that are found in many physical systems of practical importance.

Granular assemblies, a sandstone, a soil, a sand dune, are accorded special attention when they mobilize, e.g., the Big Sur mudslide [1], Loma Prieta earthquake [2], and singing sands [3]. For these systems many of the properties so revealed are conferred not by the units being assembled but by the bond system that gives the assembly structure. Laboratory samples of granular assemblies often carry properties not found in conventional materials. A Berea sandstone and in fact nearly all rocks have hysteresis and end point memory in their quasi-static response [4]; they have response to steady state drive that is a non-analytic function of the drive amplitude [5,6]. These behaviors are well studied [7] and have been known about since at least the early 1900's [8]. Less well studied are the "slow dynamics" of the transient responses of granular assemblies.

Earlier studies have reported a time-logarithmic relaxation back toward the unperturbed elastic modulus after the perturbation. The observed behavior is independent of the test material or method used: resonance frequency [6], Larsen frequency [9] or change of velocity [10]. Consequently, the handful of phenomenological models developed to describe this behavior predict a log(t) recovery [6,11]. One study [9] has presented evidence of faster than log(t) relaxation in cement paste and sandstone at early times ($t \sim 10^{-3} s$). The model proposed in [12] describes a multi-scale relaxation phenomenon that takes place on different temporal and spatial scales. The one proposed in [13] is based on the existence of metastable contacts and predicts a non logarithmic behavior at early times. Such descriptions are common to a variety of disordered mechanical systems [14,15].

Pump-probe experimental methods, in particular dynamic acousto-elastic testing (DAET), perfected over the last decade [16–19], allow us to look at the transient behavior of granular assemblies with unprecedented detail. In this paper we report the results of a pump-probe investigation of weakly consolidated granular assemblies that spans 8 orders of magnitude in time, as opposed to one or two decades in earlier studies [6,9,10]. We employ DAET to investigate the return to equilibrium of the elastic properties of rock and mortar samples that have been placed in a carefully established/controlled non-equilibrium steady state. The influences of the thermodynamic environment in which the samples are maintained and the strength of the drive, which establishes the steady state, are investigated. We present our findings in terms of a spectrum of relaxation rates that can serve as the signature of a sample.

The experimental system we employ, shown schematically in Figure 1 (left panel), is a pump-probe system. Each sample, a cylindrical specimen (L = 15-17cm, ϕ = 2.54cm), is driven in the fundamental compressional mode by a piezoelectric ceramic disk S_1 that is glued to the sample bottom and to a heavy backload. A miniature accelerometer R_1, glued to the sample top, monitors the dynamic strain field created by S_1, i.e., the pump strain field ϵ_P (ϵ_P ~ 4 x 10^{-6} and f_P ~ 4.5 kHz in Figure 1). The send-receive probe system, an ultrasonic transducer pair S_2-R_2, is positioned 2 cm above the pump source S_1. The sender S_2 (1 MHz-center frequency) broadcasts low-strain (< 10^{-7}) pulses that cross the sample to R_2 every $\Delta T = 0.1ms\ (10^{-4}s)$ throughout the experiment. The basic measurements, of the experience of the probe pulse in crossing the sample, are of the timing of the arrival of the probe pulse at R_2. These measurements, requiring high precision, make it necessary to have environmental control. As a consequence the experimental system resides in an environmental chamber that allowed temperature control (e.g., T(ºC) = 23.0 ± 0.2) and moisture control (e.g., relative humidity RH(%) = 50.0 ± 0.2).

The protocol for making measurements on a sample comprises: (1) placing the sample in the environmental chamber for at least 12 hours before testing (pump off and probe off); (2) initiate probe broadcasts at $t = 0$; (3) turn on pump at $t = 0.1s$ (the pump ring-up/ring-down time is $\sim 0.02s$); (4) keep pump on for about $1s$ after which it is turned off, $t = 1.1s$; (6) the probe, turned on at $t = 0$, is on continuously out to 30 minutes following the time when the pump is turned off.

The basic measurements, the timing of the arrival of the probe pulse at R_2, involve finding the shift in arrival time using cross-correlation methods. These shifts in time are put in the form of a relative shift in sound speed $\Delta c(t)/c_0 = (c(t) - c_0)/c_0$, where c_0 is the sound speed before the pump is turned on and $c(t)$ is the sound speed at time t. The behavior of the pump strain over the experimental protocol is shown in Fig. 1(a) and the attending behavior of the shift in sound speed is shown in Fig. 1(b). The evolution of the sound speed occurs in the six time domains marked on the figures: (1) pre-pump, (2) ring up of pump strain, (3) ring up to steady, driven elastic state (non-equilibrium steady state), (4) non-equilibrium steady state, (5) ring down of pump strain, and (6) recovery from the non-equilibrium steady state. There is partial overlap between domains 2 and 3 as well as domains 5 and 6. The slow dynamics is seen in the recovery of the sound speed in time domain 6, following the ring down of the pump strain. Careful study of the behavior of the samples in the non-equilibrium steady state, domain 4, show the non-equilibrium steady state to possess anomalous elastic properties. Here we focus on the time domain 6, $t_0 < t < t_{max}$, to examine the slow dynamics of the recovery of the system from the non-equilibrium steady state, with t_0 corresponding to the end of the ring-down of the pump strain ($t_0 = 1.12s$ in Fig. 1).

In Fig. 2(a) we show the behavior of $\Delta c(t)/c_0$ as a function of time measured from t_0. The time axis is logarithmic in order to draw attention to the many time scales involved in the recovery from the non-equilibrium steady state. To quantify the description of this recovery we introduce the concept of a *relaxation time spectrum*. The scheme to find the relaxation time spectrum is illustrated in Figure 2.

We assume the recovery of $\Delta c(t)/c_0$ to be able to be represented as a sum of discrete exponential decays each having an amplitude A_n and time constant τ_n, i.e.,

$$\zeta(t) = \sum_{n=0}^{m\times N} A_n\, e^{\frac{-t}{\tau_n}}, \quad A_n \geq 0, \tag{1}$$

where t is measured from t_0 and the time constants τ_n, which span N decades, $\Delta T \leq \tau \leq \Delta T \times 10^N$, are assigned *a priori*. The amplitudes A_n are determined by minimizing the least squares objective function

$$E = \int_{t_0}^{t_{max}} \left[\frac{\Delta c(t)}{c_0} - \zeta(t)\right]^2 dt \tag{2}$$

We choose τ_n such that there are m logarithmically spaced time constants in each decade:

$$\tau_n = \Delta T b^n,\ b = 10^{\frac{1}{m}},\ n = 0, \dots, m\times N \tag{3}$$

What results from this procedure is the set of amplitudes $A_0, A_1, \dots, A_n$, the spectrum of values of A (see Figures 2a and 2b). We find that $m = 1$ (one exponential per decade) provides an optimal fit. Smoother spectra could likely be obtained by choosing $m > 1$, but this would require some forms of regularization to prevent overfitting. The spectrum of values of A (Figure 2c) is termed the relaxation time spectrum and is taken as the *signature* of the slow dynamics recovery process. A recovery process that goes as $\log(t)$ implies a relaxation time spectrum that is featureless; no characteristic time or rate can be extracted, the relaxation spectrum is flat ($A_0 \sim A_1 \sim \dots \sim$). Earlier studies [6], that typically found $\log(t)$ behavior for the recovery process, were based on measuring the evolution of a resonance frequency. Such studies, necessarily limited by the time to sweep over a resonance, typically involve $t > 10s$. Using DAET we are able to look deep inside $10s$, at 5 orders of magnitude of time down to $t = 10^{-4}s$. Thus we are able to determine the relaxation time spectrum that characterizes the recovery process over 8 orders of magnitude, from $\Delta T = 10^{-4}s$ out to $10^{4}s$.

We have made measurements on a variety of samples in a variety of circumstances [19]. We begin with measurements on a sample of Berea sandstone at T = 23.0 ± 0.2 ºC and RH = 50.0 ± 0.2 %. In Fig. 3a we show $\Delta c(t)/c_0$ for $10^{-4}s < t < 10^{4}s$ and seven different pump strain amplitudes. The relaxation time spectra found from these data, shown in Figure 3b, are essentially independent of the pump strain amplitude. A prominent relaxation time near $\tau = 10^{-1}s$, independent of the pump strain amplitude, is apparent. At late times, $t > 10^{1}s$, the relaxation time spectra are approximately flat suggesting near $\log(t)$ recovery at long time, consistent with previous studies [6]. For this sample keeping the temperature constant at T = 23.0 ± 0.2 ºC we vary the moisture content (RH = 30%, 50%, 70%, and 90%). The normalized relaxation time spectra associated with the different RH are exhibited in Figure 3c. Although a change in RH affects the absolute spectral amplitudes (not shown), the essential structure of the relaxation time spectra remains largely unaffected. That is, the presence of different fluid configurations in the pore space does not importantly change the shape of the relaxation time spectrum.

In addition to Berea sandstone we have conducted measurements on several consolidated porous materials systems: Berea sandstone (a sedimentary rock), Grunnes soapstone (a metamorphic rock), Berkeley Blue Granite (a crystalline rock), and a stress-damaged mortar (the hardened mixture of sand and cement paste) [19]. At T = 23.0 ±

0.2 ºC and RH = 50.0 ± 0.2 %, the recovery of $\Delta c/c_0$ over time and the associated relaxation time spectra are shown in Fig. 4. Berea sandstone and Berkeley Blue granite have qualitatively similar relaxation time spectra in which the time scale 10^{-1}s is notable. In contrast, the relaxation time spectra of Grunnes soapstone and damaged mortar are relatively featureless from 10^{-2}s to 10^{4} s. One of the long-term goals of this work is to relate the shape of the relaxation spectra to microstructural features to unravel the underlying physical mechanisms. In future work, we will test various hypotheses on a larger series of samples, including the influence of grain size, grain size distribution, porosity and composition.

Many weakly consolidated granular materials and related systems have unusual elastic properties. Earlier evidence of these was (a) mechanical hysteresis with end point memory [4] and (b) unexpected nonlinear response of a resonant bar [6]. With the introduction of pump-probe experimental methods the picture of the elastic response of these systems has become refined. In the non-equilibrium steady state (domain 4 in Fig. 1) the nonlinear elastic properties, captured by the nonlinear elastic constants or hysteretic behavior, are changed quantitatively and qualitatively. While the β coefficient, the traditional measure of cubic nonlinearity, is found to be independent of the *amplitude* and *the frequency* of the pump strain field [19,20], the other nonlinear components (related to the averaged softening and hysteresis) do depend on both. The pump strain field brings about a profound change in the elastic properties of the system. Here we report the use of pump-probe methods to measure/characterize the recovery of these systems from the anomalous state established by the pump strain field, i.e., the non-equilibrium steady state. Fluid configurations in a porous media system are able to exert forces that are equivalent to an applied stress of tens of MPa [7,21]. We find that the forces brought to bear by fluid configurations pretty much leave the non-equilibrium steady state unchanged. Similarly, changes in the amplitude of the pump strain field bring about changes in the amplitude of the non-equilibrium steady state but not changes in its character; it decays in much the same way but from larger amplitude. The decay of the changes produced by the pump strain field occurs over many orders of magnitude in time. Almost 75% of the changes leave the system on the time scale of the ring-down of the driving field. Approximately 20% occurs on the time scale we are able to examine, from 10^{-2}s to 10^{4}s, and the remainder, in the noise in Fig. 2(a), can be assigned to $\log(t)$. The pump strain field causes robust changes in the elastic state of the system that do not leave the system immediately on their cause being removed.

Evidence for similar behavior is found in many systems across many scales for example in granular media [22], damaged consolidated granular media [23], and concrete [24]. A sudden drop and partial or full recovery of seismic velocities following a strong ground motion event is a widespread phenomenon at field scale [25–28]. Other examples include the co-seismic decrease and subsequent relaxation of the fundamental resonance frequencies of intact buildings [29]. Permeability was also observed to relax after modifications in effective stress field caused by pore pressure oscillations aimed at e.g., dynamic permeability enhancement vital to energy recovery applications [30].

The pump strain field is the carefully controlled laboratory realization of the, transient, incoherent, elastic noise fields in which many granular media systems are awash, e.g., a formation adjacent to a borehole, a bridge pier, a segment of a fault system. From pump-probe measures of the modified elastic state and of the persistence of that elastic state over time we learn that these systems are not simply passively moving toward a critical state. They are continually driven dynamically, having a stochastic component to their character that makes deterministic characterization difficult.

Acknowledgements

This work was supported by a grant from the DOE Office of Basic Energy Science (DE-SC0017585) to PS. JR was supported by a Marie-Curie Fellowship (Award number 655833) from the European Research Council. PAJ and RAG gratefully acknowledge support from the DOE Office of Basic Energy Science.

References

[1] C. J. Hapke and K. R. Green, Geology **34**, 1077 (2006).
[2] B.-H. Chin and K. Aki, Bull. Seismol. Soc. Am. **81**, 1859 (1991).
[3] A. J. Patitsas, J. Fluids Struct. **17**, 287 (2003).
[4] R. A. Guyer, K. R. McCall, and G. N. Boitnott, Phys. Rev. Lett. **74**, 3491 (1995).
[5] J. A. T. Cate and T. J. Shankland, Geophys. Res. Lett. **23**, 3019 (1996).
[6] J. A. TenCate, E. Smith, and R. A. Guyer, Phys. Rev. Lett. **85**, 1020 (2000).
[7] R. A. Guyer and P. A. Johnson, *Nonlinear Mesoscopic Elasticity: The Complex Behaviour of Rocks, Soil, Concrete* (John Wiley & Sons, 2009).
[8] F. D. Adams and E. G. Coker, *An Investigation Into the Elastic Constants of Rocks: More Especially with Reference to Cubic Compressibility* (Carnegie Institution of Washington, 1906).
[9] O. I. Lobkis and R. L. Weaver, J. Acoust. Soc. Am. **125**, 1894 (2009).
[10] N. Tremblay, E. Larose, and V. Rossetto, J. Acoust. Soc. Am. **127**, 1239 (2010).
[11] O. O. Vakhnenko, V. O. Vakhnenko, and T. J. Shankland, Phys. Rev. B **71**, (2005).
[12] R. Snieder, C. Sens-Schönfelder, and R. Wu, Geophys. J. Int. **208**, 1 (2017).
[13] P. A. Johnson, A. Lebedev, L. Ostrovsky, and J. Rivière, in *20th Int. Symp. Nonlinear Acoust.* (Lyon, France, 2015).
[14] A. Amir, S. Borini, Y. Oreg, and Y. Imry, Phys. Rev. Lett. **107**, 186407 (2011).
[15] Y. Lahini, O. Gottesman, A. Amir, and S. M. Rubinstein, Phys. Rev. Lett. **118**, 085501 (2017).
[16] G. Renaud, S. Callé, and M. Defontaine, Appl. Phys. Lett. **94**, 011905 (2009).
[17] G. Renaud, M. Talmant, S. Callé, M. Defontaine, and P. Laugier, J. Acoust. Soc. Am. **130**, 3583 (2011).
[18] J. Rivière, G. Renaud, R. A. Guyer, and P. A. Johnson, J. Appl. Phys. **114**, 054905 (2013).
[19] J. Rivière, P. Shokouhi, R. A. Guyer, and P. A. Johnson, J. Geophys. Res. Solid Earth **120**, 1587 (2015).

[20] J. Rivière, L. Pimienta, M. Scuderi, T. Candela, P. Shokouhi, J. Fortin, A. Schubnel, C. Marone, and P. A. Johnson, Geophys. Res. Lett. **43**, 3226 (2016).
[21] A. H. Kim and R. A. Guyer, *Nonlinear Elasticity and Hysteresis: Fluid-Solid Coupling in Porous Media* (John Wiley & Sons, 2014).
[22] T. Brunet, X. Jia, and P. A. Johnson, Geophys. Res. Lett. **35**, (2008).
[23] M. Scalerandi, M. Griffa, P. Antonaci, M. Wyrzykowski, and P. Lura, J. Appl. Phys. **113**, 154902 (2013).
[24] P. Shokouhi, J. Rivière, C. R. Lake, P.-Y. Le Bas, and T. J. Ulrich, Ultrasonics **81**, 59 (2017).
[25] E. H. Field, P. A. Johnson, I. A. Beresnev, and Y. Zeng, Nature **390**, 599 (1997).
[26] J. E. Vidale and Y.-G. Li, Nature **421**, 524 (2003).
[27] F. Brenguier, M. Campillo, C. Hadziioannou, N. M. Shapiro, R. M. Nadeau, and E. Larose, Science **321**, 1478 (2008).
[28] C. Wu, A. Delorey, F. Brenguier, C. Hadziioannou, E. G. Daub, and P. Johnson, Geophys. Res. Lett. **43**, 6129 (2016).
[29] P. Guéguen, P. Johnson, and P. Roux, J. Acoust. Soc. Am. **140**, 582 (2016).
[30] J. E. Elkhoury, E. E. Brodsky, and D. C. Agnew, Nature **441**, 1135 (2006).

Figure Captions

Figure 1: Schematic DAET setup and typical results: (a) pump strain time history from R_1; (b) associated sound velocity change from $S_2 - R_2$. The numbers mark the six time domains in the evolution of the state of the sample.

Figure 2: The scheme to find the relaxation time spectrum from the sound velocity evolution in domain 6: (a) the data is sampled and fit by a sum of exponential decays with amplitude to be determined; (b) a set of 7 exponential decay terms; (c) the amplitude of the 7 exponential decays in (b). The fit ζ is shown in (a).

Figure 3: The recovery of Berea sandstone from non-equilibrium steady state set by different pump strain amplitudes: (a) $\Delta c/c_0$ versus time t for $t > t_0$ (time axis is logarithmic); (b) ‘relaxation time spectrum’ for recovery shown in (a) [these spectra are normed

to 1, $\sum A_n = 1$]; (c) Normalized relaxation time spectrum for Berea sandstone for various relative humidity (RH). The pump strain amplitude is indicated in the legend. Note that the overall shape of the spectra is unaffected by the change in RH.

Figure 4: The recovery from the non-equilibrium steady state for Grunnes soapstone, Berea sandstone, Berkeley Blue granite and damaged mortar: (a) Velocity change $\Delta c/c_0$ versus time t; (b) the relaxation time spectra from the data in (a) [these spectra are normed to 1, $\sum A_n = 1$].

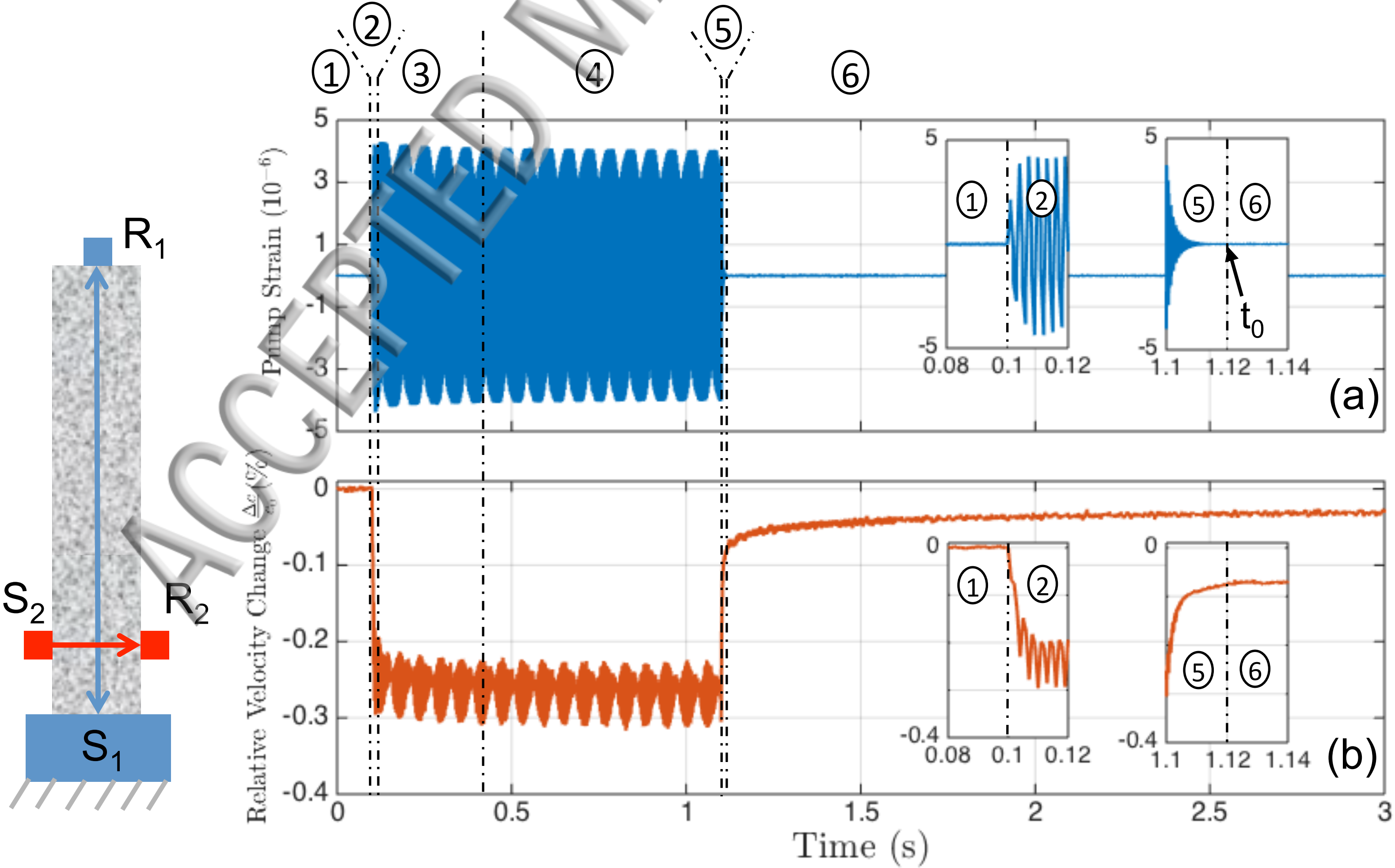
R1
R2
S1
S2
1
2
3
4
5
6
Pump Strain (10^−6)
Relative Velocity Change Δc/c0 (%)
Time (s)
t0
(a)
(b)
0
0.5
1
1.5
2
2.5
3
0.08
0.1
0.12
1.1
1.12
1.14
5
3
1
-1
-3
-5
0
-0.1
-0.2
-0.3
-0.4

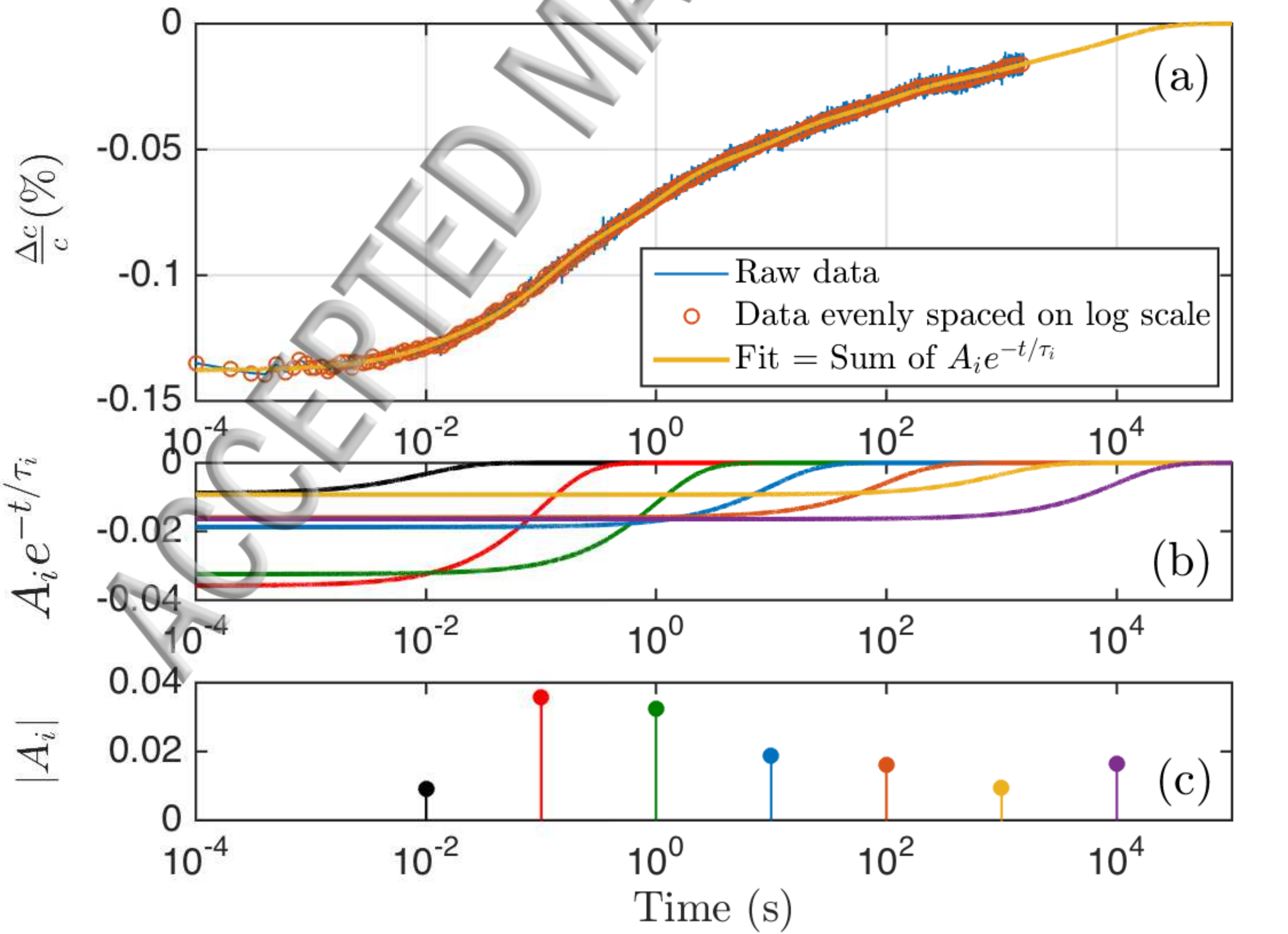

0
-0.05
-0.1
-0.15
$\frac{\Delta c}{c}(\%)$
(a)
Raw data
Data evenly spaced on log scale
Fit = Sum of $A_i e^{-t/\tau_i}$
10^{-4}
10^{-2}
10^{0}
10^{2}
10^{4}
0
-0.02
-0.04
$A_i e^{-t/\tau_i}$
(b)
10^{-4}
10^{-2}
10^{0}
10^{2}
10^{4}
0.04
0.02
0
$|A_i|$
(c)
10^{-4}
10^{-2}
10^{0}
10^{2}
10^{4}
Time (s)

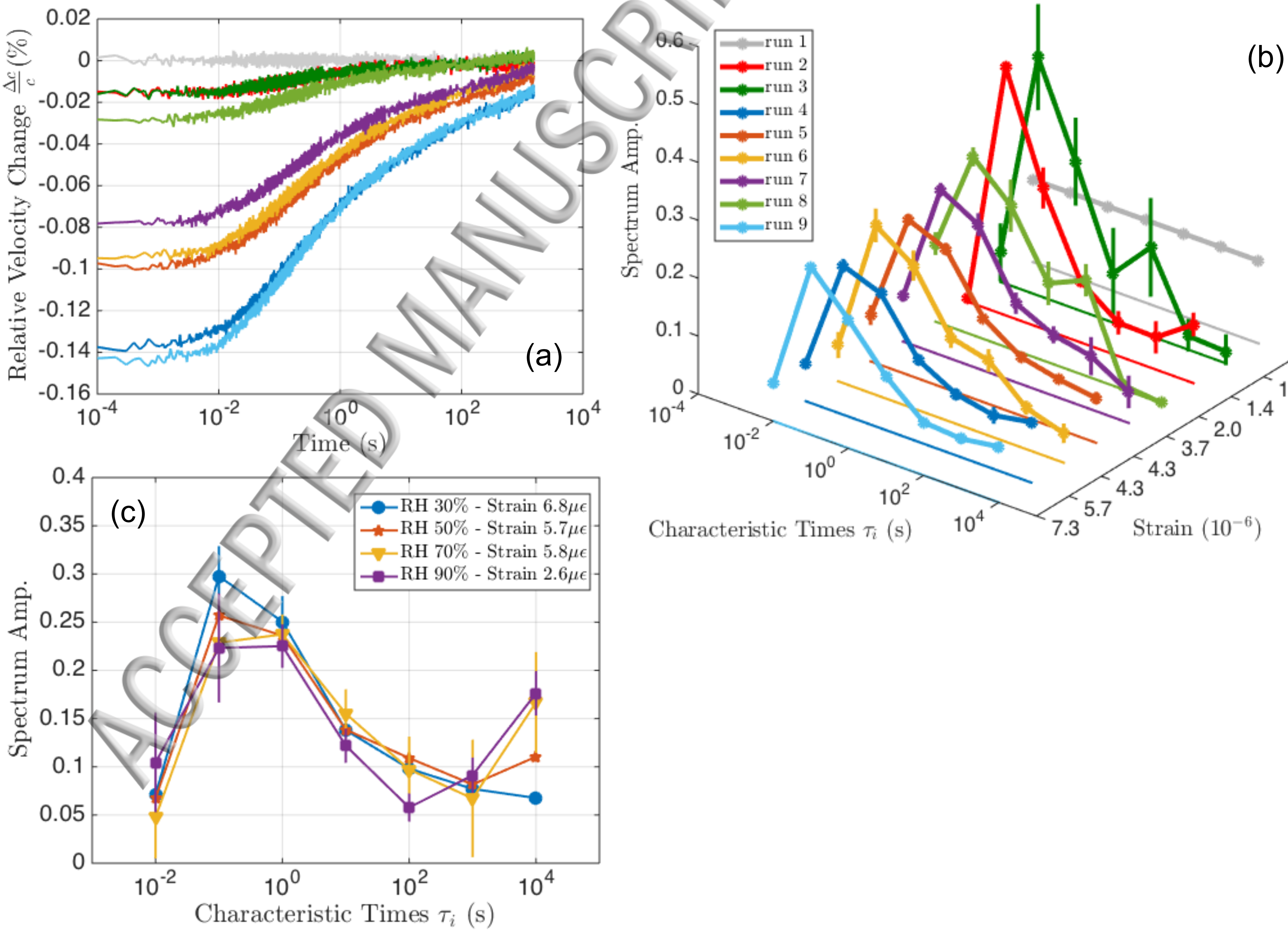
(a)
Relative Velocity Change $\frac{\Delta c}{c}$ (%)
Time (s)
0.02
0
-0.02
-0.04
-0.06
-0.08
-0.1
-0.12
-0.14
-0.16
10^{-4}
10^{-2}
10^{0}
10^{2}
10^{4}
(b)
Spectrum Amp.
run 1
run 2
run 3
run 4
run 5
run 6
run 7
run 8
run 9
Characteristic Times τ_i (s)
Strain (10^{-6})
0.0
1.4
1.4
2.0
3.7
4.3
4.3
5.7
7.3
(c)
Spectrum Amp.
Characteristic Times τ_i (s)
RH 30% - Strain 6.8$\mu\epsilon$
RH 50% - Strain 5.7$\mu\epsilon$
RH 70% - Strain 5.8$\mu\epsilon$
RH 90% - Strain 2.6$\mu\epsilon$

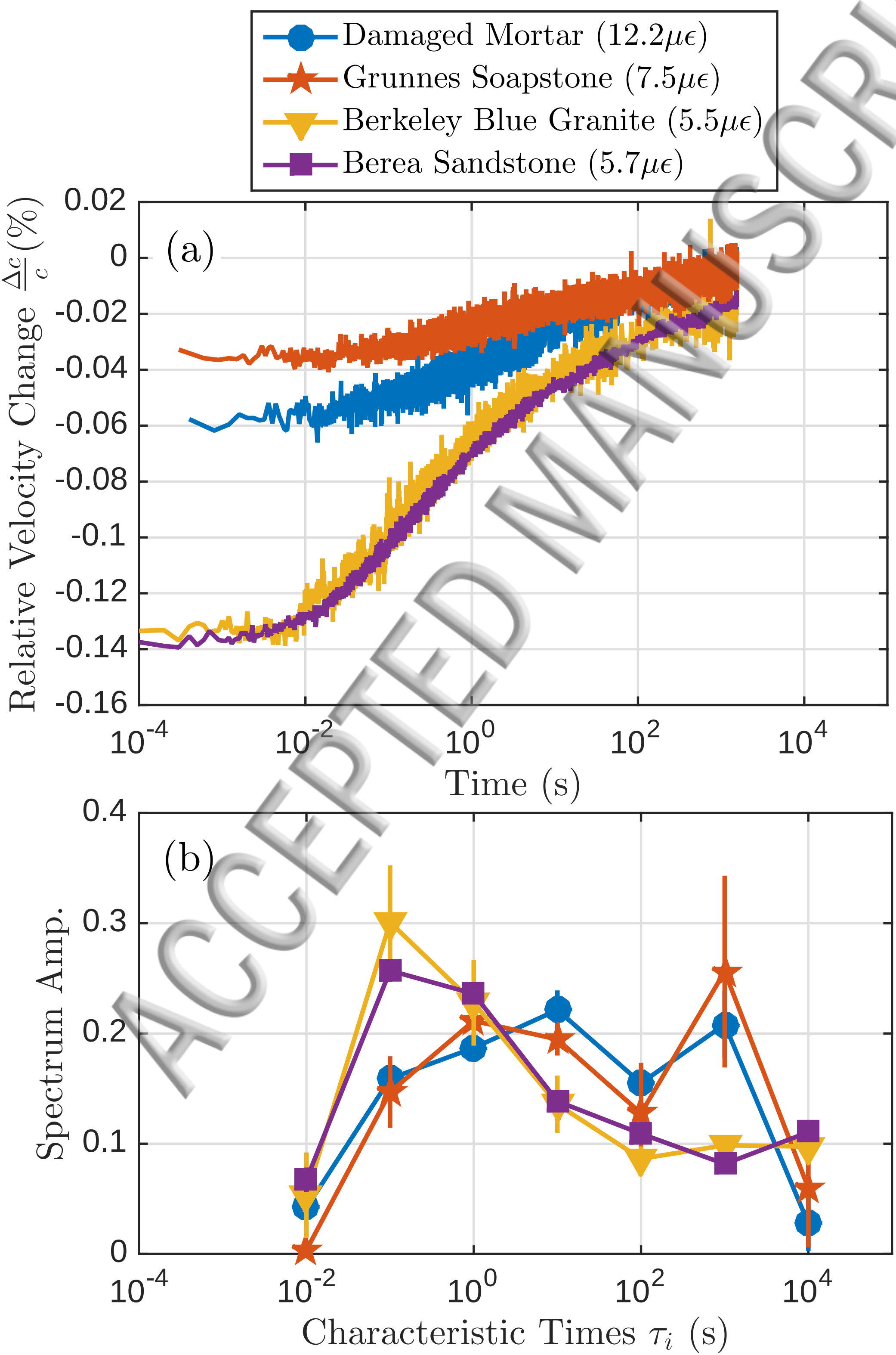

Damaged Mortar (12.2$\mu\epsilon$)
Grunnes Soapstone (7.5$\mu\epsilon$)
Berkeley Blue Granite (5.5$\mu\epsilon$)
Berea Sandstone (5.7$\mu\epsilon$)
(a)
Relative Velocity Change $\frac{\Delta c}{c}$(%)
0.02
0
-0.02
-0.04
-0.06
-0.08
-0.1
-0.12
-0.14
-0.16
10^{-4}
10^{-2}
10^{0}
10^{2}
10^{4}
Time (s)
(b)
Spectrum Amp.
0.4
0.3
0.2
0.1
0
10^{-4}
10^{-2}
10^{0}
10^{2}
10^{4}
Characteristic Times τ_i (s)